Elasticity model for the evaluation of structural parameters in multilayer systems with applications to transition metal and Si-based multilayers

Mikael Råsander,* Petros Souvatzis, Andreas Höglund, and Olle Eriksson
Department of Physics and Astronomy, Divison for Materials Theory, Box 516, Uppsala University, SE-75120 Uppsala, Sweden
(Received 15 December 2010; revised manuscript received 2 August 2011; published 9 September 2011)

In this paper we present and evaluate a model based on elasticity theory for the calculation of in- and out-of-plane lattice parameters in multilayer systems, which can be used for a wide selection of multilayers. The model assumes perfect lattice matching at the interface between the different components in the multilayer. The only input is the knowledge of the elastic and lattice constants of the different components in the bulk as well as the relative thickness between the components in the multilayer. We show that the model is in good agreement when compared to first-principles theory calculations and also that there is good agreement between the model and experimental structures for several multilayer systems. The model is also shown to be more appropriate in describing thicker multilayers with larger periodicities such that the lattice constants in the system are independent on the periodicity. Furthermore, we provide results for the lattice parameters for a large body of multilayers based on transition metals and semiconducting materials.

DOI: 10.1103/PhysRevB.84.125424 PACS number(s): 68.65.Ac, 68.65.Cd

I. INTRODUCTION

The ability to grow materials, layer by layer, in a controlled way, has opened new opportunities and challenges in materials research. It is now well established that almost all combinations of elements can be grown on top of each other, often epitaxially, i.e., in such a way that the same basic crystal structure is preserved as one crosses the interface between one element type to the next. One of the most frequently studied classes of such human-made materials is the so-called multilayer structure illustrated in Fig. 1. Part of the interest in these systems is that by careful choice of components in the multilayer, new and improved functionality can be obtained. An example of this is the magnetic multilayers displaying the giant magnetoresistance (GMR) effect. Typically magnetic and nonmagnetic elements are chosen for the growth of a magnetic multilayer, and, in combination with the unexpected interlayer exchange coupling, the equally surprising GMR effect was demonstrated.[1,2] Other examples of where the fabrication of multilayer structures have led to new or extreme properties are the supermodulus effect, materials with dislocation blocking under external strain,[3] as well as quantum well states in semiconductors.[4] Recently, it has further been suggested that the equilibrium doping solubility in III-V semiconductors can be increased by the formation of multilayers.[5]

Experimentally the functionality of a multilayer has been found to be coupled to its structural properties. Via experimental techniques such as x-ray diffraction and neutron scattering experiments one can obtain information about the in-plane lattice constant and the average out-of-plane lattice constant of the multilayer (i.e., the average over all atomic planes of the out-of-plane lattice constant). Often one observes a very strong coupling between structural arrangement of the atomic species and the functionality of the material. Possibly the best example of this coupling is Fe, which is a ferromagnetic material in the body-centered cubic phase and a nonmagnetic (or noncollinear magnetic) material in the face-centered cubic phase. For this reason it becomes important to not only have accurate measurements of the crystal structure of these multilayers but also to have accurate theoretical tools, preferably with predictive power. Density functional theory is indeed such a tool, and it is by now well established that the crystal structure of almost any element, compound, or multilayer is well reproduced by this theory.[6] Unfortunately, such calculations can be quite time-consuming, especially for multilayer systems where the number of atoms necessary for the calculation is large. Hence simpler and more efficient methods are needed.

We explore in this paper a simple and fast approach for obtaining information about the structural properties of multilayers. The method relies on the theory of elasticity in general and is expected to be accurate if the introduction of interfaces, as indeed is done in multilayers, does not influence the chemical bonding in a significant way. Hence we expect our method to be accurate for thicker multilayers or for multilayers where the electronic structure of the interface atoms is not significantly altered from that of more bulk like atoms of the multilayer. A preliminary study relying on this approach has been published in Ref. 7. Here we will present the model and test it against first-principles theory calculations for different multilayers. Furthermore, we have performed calculations of a large number of different metallic and semiconducting multilayers, the results of which are presented here and will serve as a structural database.

The rest of this paper is organized as follows. In Sec. II we provide the details of our theoretical model. In Sec. III we present the general features of the model using the example of a V/Cr multilayer and evaluate its performance compared to structures obtained using first-principles density functional theory calculations, we will also present structural parameters obtained using our model for a large set of various multilayers, and in Sec. IV we will summarize our results and draw conclusions.

II. THEORY

We calculate the lattice parameters of the multilayer by use of an analytical model where the energy of the multilayer

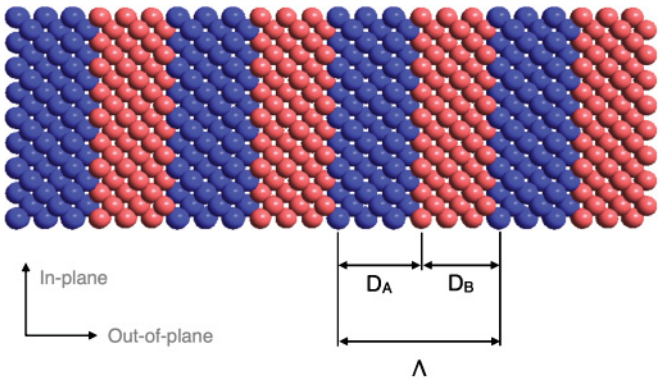

FIG. 1. (Color online) Schematic illustration of a multilayer structure, composed of two different atomic species, symbolized by red and blue spheres. D_A and D_B are the thickness of layer A and B respectively, and Λ is the periodicity. The arrows shows the in- and out-of-plane directions of the multilayer.

structure is expressed as the sum of the energy from each material building up the multilayer, i.e.,

$$E_{\text{tot}} = E_A + E_B, \tag{1}$$

where $E_{\text{A/B}}$ is the total energy of the multilayer component A/B. The energy of each multilayer component is expressed as contributions from strain along the epitaxial growth direction, with corresponding strain in the perpendicular direction, and volume distortions. For the case of cubic geometry multilayers this corresponds to the tetragonal and volume distortions of the cubic cell of each of the materials building up the multilayer. We also assume that the multilayers are perfectly lattice matched at the interface. The total energy of the system is then the sum of the two constituent multilayers and the most stable structure is given by the minimum of this total energy with respect to changes in the lattice parameters. In this way the overall structure is determined solely by the elastic constants of the material in each component of the multilayer.

We now focus on the case of cubic crystals making up the multilayer and that the interface between the different components is any of the (100), (010), or (001) surfaces. For this case the energy contribution from the tetragonal distortion can be written as

$$E_s = E_0 + 6c'\delta^2 V, \tag{2}$$

where the tetragonal shear constant c' is related to the elastic constants c_{11} and c_{12} and δ is defined via the c/a ratio as

$$\frac{c}{a} = \frac{1}{(1+\delta)^3}. \tag{3}$$

Furthermore, the energy for a change in volume can be expressed as

$$E_v = E_0 + \frac{\partial E_v}{\partial V}\Delta V + \frac{1}{2}\frac{\partial^2 E_v}{\partial V^2}(\Delta V)^2 + \cdots, \tag{4}$$

where the first term corresponds to the equilibrium volume, the second term is zero since the distortion is made from an equilibrium configuration, and the third term is related to the bulk modulus, B. The change in volume is given by

$$\Delta V = \left(a_\perp a_\parallel^2 - a_0^3\right), \tag{5}$$

TABLE I. Experimental bulk lattice parameters (a), elastic constants (c_{ij}), tetragonal shear constants (c'), and bulk modulus (B) for each element used in the calculations. Unless otherwise stated, the data are taken from Refs. 9 and 10. (Ga,In)As is an alloyed semiconductor with chemical formula $Ga_{0.47}In_{0.53}As$. Data within parenthesis are obtained from first-principles calculations as explained in the text.

Element	a (Å)	c_{11} (GPa)	c_{12} (GPa)	c_{44} (GPa)	c' (GPa)	B (GPa)
V	3.02 (2.98)	196 (260)[a]	133 (135)[a]	67 (17)[a]	32 (63)[a]	154 (177)[a]
Cr	2.88 (2.84)	350 (469)	68 (151)	101 (101)	141 (159)	162 (257)
Fe	2.87	237	141	116	48	173
Nb	3.30	240	126	28	57	164
Mo	3.15 (3.15)	470 (463)[a]	168 (163)[a]	107 (103)[a]	151 (150)[a]	268 (263)[a]
Ta	3.31	261	157	82	52	192
W	3.16	523	205	161	159	311
Ni	3.52	251	150	124	50	184
Cu	3.61	168	121	75	23	137
Rh	3.80	413	194	184	110	267
Pd	3.89	227	176	72	26	193
Ag	4.09	124	94	47	15	104
Ir	3.84	580	242	256	169	355
Pt	3.92	347	251	77	48	283
Au	4.08	193	164	42	15	174
Si	5.43	160	64	80	50	97
Ge	5.66	130	44	68	41	71
GaAs	5.65	120	53	60	33	75
InP	5.87	100	56	46	22	71
InAs	6.06	83	45	39	19	58
InSb	6.48	67	37	30	15	47
GaP	5.45	140	62	70	39	88
(Ga,In)As	5.87	100	49	49	25	66

[a]The first principles elastic constants of V and Mo is taken from Ref. 17.

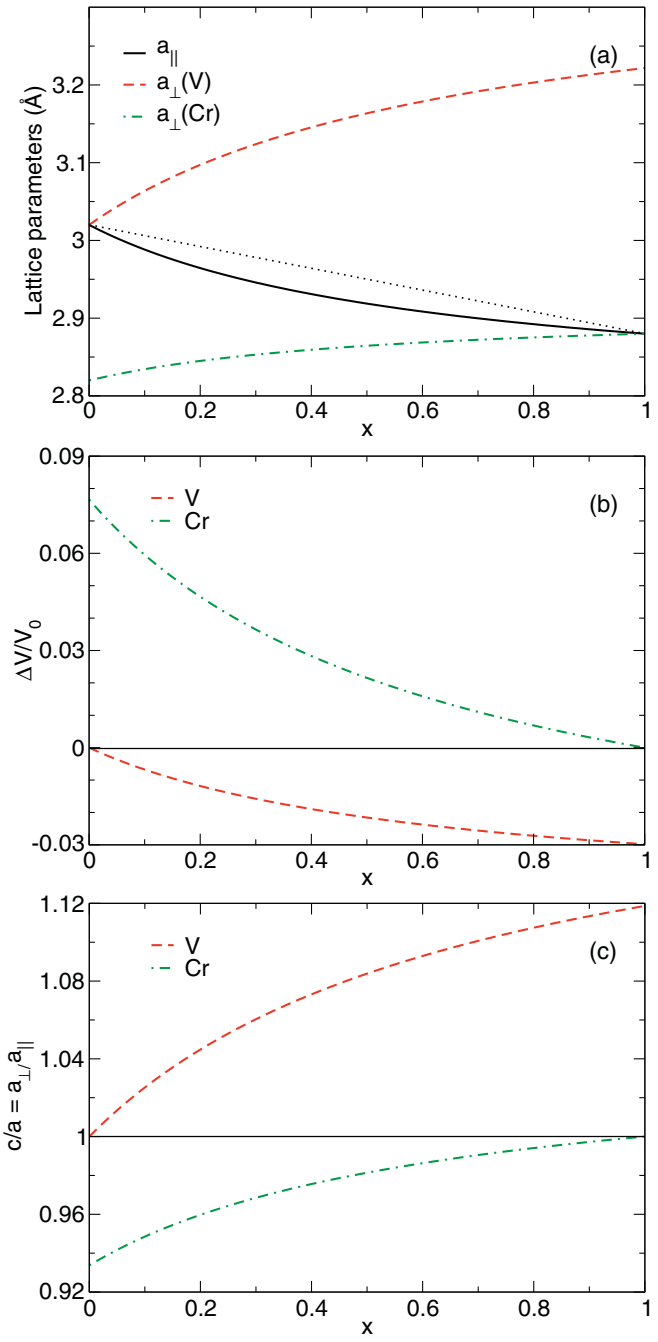

FIG. 2. (Color online) Calculated in- ($a_\parallel$) and out-of-plane ($a_\perp$) lattice parameters for V/Cr multilayers (a), relative changes in volume (b), and c/a ratios (c) as obtained by our model. In (a) the solid (black) curve is the in-plane lattice parameter and the dashed (red) and semidotted (green) curves are the out-of-plane lattice parameter for the V and Cr layers, respectively. The dotted (black) line is the expected behavior derived from Vegards law. The data for the relative changes in volume and c/a ratios for V and Cr layers is given by the dashed (red) and semidotted (green) curves, respectively, in both (b) and (c). All curves are given as a function of the relative concentration of Cr, X, defined in Eq. (8).

where $a_\parallel$ and $a_\perp$ are the lattice parameters of the tetragonally strained layers in and out of plane, respectively, where the geometry refers to the plane of the interface between the different layers (see Fig. 1) and a_0 is the lattice parameter of the unstrained cubic crystal. For actual calculations, c' and B are taken to be the bulk values of the constituent materials. This is a reasonable approximation for relatively thick multilayers. However, it has been shown that for multilayer thicknesses of down to ∼2 Å, the model still gives close agreement to experiment.[7]

The change in total energy of a component in the multilayer is then given by

$$E_i = E_0 + 6c'\left[\left(\frac{a_\parallel}{a_\perp}\right)^{1/3} - 1\right]^2 a_0^3 + \frac{B}{2a_0^3}\left(a_\perp a_\parallel^2 - a_0^3\right)^2. \tag{6}$$

For a multilayer consisting of N_A layers of material A and N_B layers of material B, the total energy is

$$E_{\text{tot}} = N_A E_A + N_B E_B. \tag{7}$$

The equilibrium configuration is finally found by minimizing the energy with respect to the lattice parameters $a_\parallel$, $a_\perp^A$, and $a_\perp^B$, where the A and B superscripts are introduced to denote the out-of-plane lattice parameters in the different multilayer components.

It is now possible to calculate the lattice parameters for any multilayer system composed of elements or alloys with cubic symmetry as illustrated in Fig. 1. This model was previously tested for Fe/V multilayers[7,8] with good agreement with experiments. We note here that with this model one would obtain the same structural parameters for an A_{N_A}/B_{N_B} multilayer as for an A_{2N_A}/B_{2N_B} multilayer, since we consider ideal crystalline lattices without defects. This means that the model is less applicable in the ultrathin limit when N_A or N_B is in the range of 1 or 2. The model is also not applicable in the limit of N_A or N_B approaching bulk values. We also note that the model is at this stage only appropriate for multilayers with a 001 orientation. For other geometries or orientations it is necessary to modify the expressions above, although the basic idea would be the same. Since the model gives the same structural parameters for multilayers with the same relative thickness of components A and B, we have chosen to present the calculated data for the various multilayers in terms of the relative concentration of the different materials in the multilayer, where the relative concentration of material B is given by

$$X = \frac{N_B}{N_A + N_B}. \tag{8}$$

Furthermore, we note that this model gives access to the out-of-plane lattice constants for each component in the multilayer. However, this information is not available in experiments since an x-ray diffraction measurement, for example, will measure only the average out-of-plane lattice constant, $\langle a_\perp \rangle$, which for an A_{N_A}/B_{N_B} multilayer is given by

$$\langle a_\perp \rangle = \frac{N_A a_\perp^A + N_B a_\perp^B}{N_A + N_B} \tag{9a}$$

$$= \frac{D_A + D_B}{N_A + N_B}, \tag{9b}$$

where D_A and D_B are the thickness of each component in the multilayer.

TABLE II. In-plane ($a_\parallel$) and out-of-plane ($a_\perp$) lattice parameters for Si/Ge and GaP/InP multilayers as obtained by our model and structures obtained from first-principles calculations. DFT means that the lattice constants are evaluated for multilayer geometries using first-principles calculations while exp means that the results is obtained using the elasticity model with experimental elastic constants as input. All lattice constants are given in Å. The data for multilayer structures from DFT have been taken from Ref. 5.

$A_{1-x}B_x$	$a_\parallel$ (DFT)	$a_\perp^A$ (DFT)	$a_\perp^B$ (DFT)	$a_\parallel$ (exp)	$a_\perp^A$ (exp)	$a_\perp^B$ (exp)
$Si_{0.5}Ge_{0.5}$	5.50	5.30	5.71	5.53	5.35	5.75
$(GaP)_{0.67}(InP)_{0.33}$	5.68	5.10	5.97	5.69	5.24	6.08
$(GaP)_{0.5}(InP)_{0.5}$	5.61	5.17	6.05	5.62	5.30	6.17
$(GaP)_{0.33}(InP)_{0.67}$	5.54	5.24	6.12	5.55	5.37	6.25

III. RESULTS AND DISCUSSION

We have performed a series of calculations of the lattice parameters for cubic metals and semiconducting multilayer systems. Experimental elastic constants and lattice parameters used in these calculations are shown in Table I. The results are collected and presented in Tables II to XVIII. However, we begin the presentation of our results with a discussion of the general features of the multilayer model.

In Fig. 2 we present, as an example, the results for a V/Cr multilayer calculation, as a function of the relative concentration of Cr. As expected, the in-plane and out-of-plane lattice parameter coincides with the bulk lattice parameter of 3.02 Å for V when there is no Cr present, i.e., for $X = 0$. Similarly, when there is no V in the multilayer, corresponding to $X = 1$, the lattice parameters becomes the same as that of bulk Cr (2.88 Å). For cases when both V and Cr are present in the multilayer, and with increasing relative concentration of Cr, the in-plane lattice parameter decreases while the out-of-plane parameter increases for both the V and Cr components. This trend is general to all materials considered, when the relative concentration of the smaller component increases, the in-plane lattice constant will decrease while the out-of-plane lattice constant will increase for both components, which is evident in the case of V and Cr in Fig. 2, since Cr has a smaller lattice constant than V. A simple approximation for the lattice constants in multilayers is the assumption of Vegards law behavior,[11] i.e., a linear variation of the lattice constants as a function of the relative concentration of the different species. It is clear from Fig. 2 that the model deviates from a linear type of behavior. This deviation is especially noticeable for the out-of-plane lattice parameters.

An important observation is that the distortions are not volume conserving. To illustrate this we show in Fig. 2 the relative change in volume of the Cr and V layers. The relative change in volume is obtained by dividing Eq. (5) by the equilibrium volume V_0 of the respective bulk component. From the results shown in Fig. 2 it is seen that the relative volume change lies in the range of 0–3 % for V and 0–8 % for Cr, depending on the relative amount of V and Cr. We also note that as the amount of Cr increases, the volume of the V layers decreases while the volume of the Cr component increases compared to the bulk value when put in a multilayer with V. It is clear from the results presented in Fig. 2 that the volume of each element of the multilayer is not conserved when varying the composition. The fact that the relative change of the volume of the Cr component is larger than the corresponding change for V is due to the size difference between bulk V and bulk Cr since the bulk modulus, B, of each metal is only slightly larger for Cr than for V; see Table I.

We also show in Fig. 2 the tetragonal distortion for each element in the V/Cr multilayer for various relative concentration. The distortion from cubic symmetry is given by the c/a ratio of each component in the multilayer. Important to note is that the c axis in the model is identical to the out-of-plane direction. According to our convention the tetragonal distortion will therefore be smaller than unity when the out-of-plane lattice constant, $a_\perp$, is smaller than the in-plane constant, $a_\parallel$, which is the case for the Cr component as shown in Fig. 2. Compared to the changes in the volume, the tetragonal distortions are found to be larger, of the order of 0–12% for the V layer and 0–7% for the Cr layer. These distortions are typical for most of the materials studied by us here. In this case the c/a ratio varies more for V than for Cr, which is reflected in the difference in each metals value for the tetragonal shear constant as shown in Table I.

We also note that the curvature of the lattice parameters shown in Fig. 2 are greater for low concentrations of Cr,

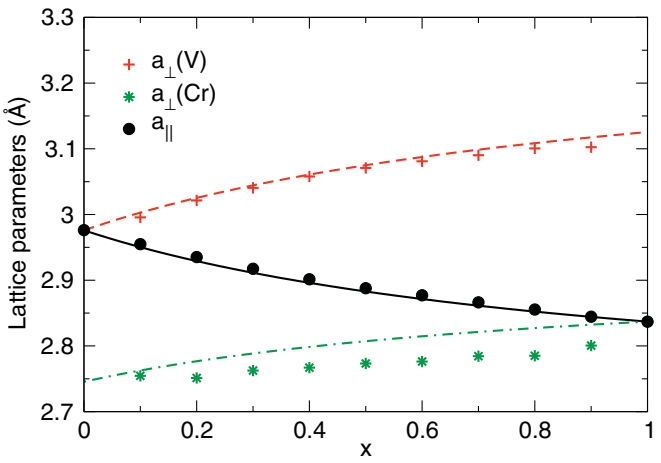

FIG. 3. (Color online) Calculated in- ($a_\parallel$) and out-of-plane ($a_\perp$) lattice parameters for V/Cr multilayers obtained by first-principles theory compared to our model calculation based on elastic constants and bulk lattice constants for V and Cr obtained by first-principles calculations. The full (black) line is the in-plane lattice constant, while the dashed (red) and semidotted (green) lines are the out-of-plane lattice constants for V and Cr, respectively, as obtained by the model calculation. For the first-principles data the in-plane lattice constant is shown with (black) full circles, while the out-of-plane constants are shown using (red) crosses and (green) stars for V and Cr, respectively.

TABLE III. Calculated structural parameters of V/A multilayers, where A is Cr, Nb, Mo, Ta, and W. The first column shows the relative concentration of material A in the multilayer. The in- and out-of-plane lattice constants are given in Å.

	V/Cr			V/Nb			V/Mo			V/Ta			V/W		
X	$a_{\parallel}^{V/Cr}$	$a_{\perp}^{V}$	$a_{\perp}^{Cr}$	$a_{\parallel}^{V/Nb}$	$a_{\perp}^{V}$	$a_{\perp}^{Nb}$	$a_{\parallel}^{V/Mo}$	$a_{\perp}^{V}$	$a_{\perp}^{Mo}$	$a_{\parallel}^{V/Ta}$	$a_{\perp}^{V}$	$a_{\perp}^{Ta}$	$a_{\parallel}^{V/W}$	$a_{\perp}^{V}$	$a_{\perp}^{W}$
0.00	3.020	3.020		3.020	3.020		3.020	3.020		3.020	3.020		3.020	3.020	
0.10	2.988	3.063	2.836	3.063	2.962	3.561	3.057	2.971	3.216	3.064	2.962	3.632	3.062	2.964	3.236
0.20	2.964	3.097	2.845	3.101	2.913	3.517	3.081	2.939	3.199	3.103	2.911	3.577	3.089	2.929	3.216
0.30	2.946	3.124	2.853	3.136	2.870	3.478	3.098	2.917	3.187	3.138	2.867	3.529	3.107	2.905	3.201
0.40	2.931	3.145	2.859	3.166	2.833	3.444	3.111	2.901	3.178	3.170	2.829	3.487	3.121	2.888	3.190
0.50	2.919	3.163	2.864	3.194	2.800	3.414	3.121	2.888	3.170	3.199	2.794	3.449	3.131	2.876	3.182
0.60	2.908	3.179	2.869	3.219	2.770	3.386	3.129	2.878	3.165	3.225	2.764	3.416	3.140	2.865	3.176
0.70	2.900	3.192	2.872	3.242	2.744	3.361	3.136	2.870	3.160	3.249	2.736	3.385	3.146	2.857	3.171
0.80	2.892	3.203	2.875	3.263	2.721	3.339	3.141	2.863	3.156	3.271	2.712	3.358	3.152	2.851	3.167
0.90	2.886	3.213	2.878	3.282	2.699	3.319	3.146	2.857	3.153	3.291	2.689	3.333	3.156	2.845	3.163
1.00	2.880		2.880	3.300		3.300	3.150		3.150	3.310		3.310	3.160		3.160

while it is almost linear for higher concentrations. This is because the relevant elastic constants for Cr are larger than for V, hence Cr is less inclined toward structural changes and therefore forcing the V layers to change their lattices more prominently. This trend also holds in general and applies to all the materials considered.

Although relatively few degrees of freedom are used, our simple model has been found to be in close agreement to the results of first-principles electronic structure calculations. More specifically, accounting for the typical error in the equilibrium lattice constant made by first-principles theory, the elastic model presented here and first-principles calculations on multilayers performed by Höglund *et al.*[5] show an agreement to within 0.01 Å (0.03 Å) for the in-plane lattice constant and within about 0.1 Å (0.05 Å) for the out-of-plane constants in InP/GaP (Si/Ge) multilayer structures, when experimental elastic and lattice constants from Table I has been used as input to the model; see Table II. For the metallic multilayers discussed previously we will here give a detailed comparison between our model and results obtained from first-principles theory. For this reason, we have performed first-principles density functional theory calculations on a series of V/Cr and V/Mo multilayers. These calculations have been performed with the Vienna *ab initio* simulation package[12,13] using the projected augmented wave method[14] for supercells consisting of 10 and 20 atomic layers. The generalized gradient approximation[15] was used for the exchange correlation functional and we have used a k-points mesh of $20 \times 20 \times 1$ and a plane wave cutoff of 300 eV. In these calculations, we have neglected the possibility for a magnetic solution for the multilayers. There is practically no difference between our first-principles calculations made using 10 and 20 atomic layers, so in what follows the discussion will be based on the results obtained using 20 atomic layers.

In order to perform a fair comparison between our model and first-principles theory there are a few points that need to be considered. Since the model uses bulk elastic and lattice constants of the different components in the multilayer as input, its accuracy when compared to first-principles calculations of a multilayer will depend on how well the input to the model compares with bulk elastic and lattice constants obtained by first-principles calculations. It is known that first-principles calculations may over- or underestimate the lattice constants of bulk materials depending on the material and which approximation for the exchange and correlation functional that has been used. Furthermore, the

TABLE IV. Calculated structural parameters of Cr/A multilayers, where A is Nb, Mo, Ta, and W. The first column shows the relative concentration of material A in the multilayer. The in- and out-of-plane lattice constants are given in Å.

	Cr/Nb			Cr/Mo			Cr/Ta			Cr/W		
X	$a_{\parallel}^{Cr/Nb}$	$a_{\perp}^{Cr}$	$a_{\perp}^{Nb}$	$a_{\parallel}^{Cr/Mo}$	$a_{\perp}^{Cr}$	$a_{\perp}^{Mo}$	$a_{\parallel}^{Cr/Ta}$	$a_{\perp}^{Cr}$	$a_{\perp}^{Ta}$	$a_{\parallel}^{Cr/W}$	$a_{\perp}^{Cr}$	$a_{\perp}^{W}$
0.00	2.880	2.880		2.880	2.880		2.880	2.880		2.880	2.880	
0.10	2.908	2.869	3.748	2.915	2.866	3.311	2.908	2.869	3.866	2.920	2.864	3.345
0.20	2.937	2.857	3.711	2.948	2.852	3.290	2.938	2.857	3.819	2.956	2.849	3.318
0.30	2.969	2.843	3.673	2.978	2.839	3.270	2.970	2.843	3.770	2.988	2.834	3.293
0.40	3.004	2.827	3.631	3.007	2.826	3.250	3.005	2.827	3.718	3.019	2.820	3.270
0.50	3.041	2.810	3.587	3.034	2.813	3.231	3.043	2.809	3.662	3.047	2.807	3.248
0.60	3.083	2.790	3.539	3.060	2.801	3.214	3.085	2.789	3.602	3.072	2.795	3.228
0.70	3.128	2.767	3.487	3.084	2.789	3.197	3.132	2.766	3.538	3.097	2.783	3.209
0.80	3.179	2.742	3.430	3.107	2.778	3.180	3.184	2.739	3.469	3.119	2.772	3.192
0.90	3.236	2.712	3.368	3.129	2.767	3.165	3.242	2.708	3.393	3.140	2.761	3.175
1.00	3.300		3.300	3.150		3.150	3.310		3.310	3.160		3.160

TABLE V. Calculated structural parameters of Fe/A multilayers, where A is V, Cr, Nb, and W. The first column shows the relative concentration of material A in the multilayer. The in- and out-of-plane lattice constants are given in Å.

	Fe/V			Fe/Cr			Fe/Nb			Fe/W		
X	$a_{\parallel}^{\mathrm{Fe/V}}$	$a_{\perp}^{\mathrm{Fe}}$	$a_{\perp}^{\mathrm{V}}$	$a_{\parallel}^{\mathrm{Fe/Cr}}$	$a_{\perp}^{\mathrm{Fe}}$	$a_{\perp}^{\mathrm{Cr}}$	$a_{\parallel}^{\mathrm{Fe/Nb}}$	$a_{\perp}^{\mathrm{Fe}}$	$a_{\perp}^{\mathrm{Nb}}$	$a_{\parallel}^{\mathrm{Fe/W}}$	$a_{\perp}^{\mathrm{Fe}}$	$a_{\perp}^{\mathrm{W}}$
0.00	2.870	2.870		2.870	2.870		2.870	2.870		2.870	2.870	
0.10	2.881	2.857	3.220	2.871	2.868	2.881	2.920	2.811	3.734	2.939	2.790	3.331
0.20	2.893	2.843	3.202	2.873	2.867	2.881	2.969	2.757	3.675	2.989	2.734	3.293
0.30	2.905	2.828	3.183	2.874	2.865	2.881	3.015	2.706	3.619	3.028	2.692	3.263
0.40	2.919	2.813	3.164	2.875	2.864	2.881	3.060	2.658	3.566	3.059	2.659	3.239
0.50	2.933	2.797	3.143	2.876	2.863	2.881	3.104	2.614	3.515	3.084	2.634	3.219
0.60	2.948	2.780	3.121	2.877	2.862	2.880	3.146	2.572	3.468	3.105	2.613	3.203
0.70	2.964	2.762	3.098	2.878	2.861	2.880	3.186	2.533	3.422	3.122	2.596	3.190
0.80	2.981	2.743	3.073	2.879	2.860	2.880	3.225	2.496	3.380	3.136	2.581	3.178
0.90	3.000	2.722	3.047	2.879	2.859	2.880	3.263	2.461	3.339	3.149	2.569	3.169
1.00	3.020		3.020	2.880		2.880	3.300		3.300	3.160		3.160

elastic constants calculated using first-principles theory may differ compared to experiments with 5–10%.[16] In the case of Cr, V, and Mo, Table I also shows the lattice and elastic constants obtained by first-principles calculations. Here the elastic constants of V and Mo were obtained by Koči *et al.*,[17] while the data for Cr as well as the lattice constants of V and Mo are obtained by us. The elastic constants of Cr have been obtained in a similar fashion as in Ref. 17. As can be seen in Table I the bulk lattice parameters obtained by first-principles calculations underestimate the lattice constants by 0.04 Å for both V and Cr compared to the values in Table I, while there is perfect agreement in the case of Mo. At the same time, the elastic constants show substantial differences between theory and experiment for Cr and V. For the constants that are relevant for our model, c' and B, this is especially true for the tetragonal shear constant in the case of V and for the bulk modulus in the case of Cr. For Cr, these differences are attributed to the neglect of the magnetic properties of Cr, which is an antiferromagnet, in the calculation of the elastic constants. By incorporating these effects in the first-principles calculations a better agreement is obtained.[18]

Judging from these discrepancies, the best way to assess the accuracy of our model is to use first-principles calculations to obtain elastic and lattice constants and to use those as input to the model and then compare the structural properties from the model with first-principles theory of the geometry of the multilayer. The result of such a calculation for a V/Cr multilayer is shown in Fig. 3, where we have used the theoretical values listed in Table I. As is clearly shown, the model and first-principles data are in an overall good agreement. Calculations on V/Mo multilayers performed by us give similar variations as the V/Cr system discussed here and with the same overall agreement when elastic constants obtained by first-principles theory has been used in the model. Therefore we conclude that the model captures the essential behavior of the multilayer when it comes to its structure and that the influence of interface effects is in this regard not essential.

A detailed comparison between our model and experimental multilayer structures is complicated due to the interaction between the multilayer and the substrate in the experimental setup, since the substrate will affect the structural parameters in the multilayer, yielding structural parameters that slightly differ from the ones obtained by us. Therefore, in order to make a clear evaluation of the accuracy of our model, we have focused in this paper on the comparison between our model and first-principles calculations on selected multilayers.

TABLE VI. Calculated structural parameters of Nb/A multilayers, where A is Mo, Ta, and W. The first column shows the relative concentration of material A in the multilayer. The in- and out-of-plane lattice constants are given in Å.

	Nb/Mo			Nb/Ta			Nb/W		
X	$a_{\parallel}^{\mathrm{Nb/Mo}}$	$a_{\perp}^{\mathrm{Nb}}$	$a_{\perp}^{\mathrm{Mo}}$	$a_{\parallel}^{\mathrm{Nb/Ta}}$	$a_{\perp}^{\mathrm{Nb}}$	$a_{\perp}^{\mathrm{Ta}}$	$a_{\parallel}^{\mathrm{Nb/W}}$	$a_{\perp}^{\mathrm{Nb}}$	$a_{\perp}^{\mathrm{W}}$
0.00	3.300	3.300		3.300	3.300		3.300	3.300	
0.10	3.271	3.331	3.063	3.301	3.299	3.321	3.271	3.331	3.074
0.20	3.247	3.356	3.080	3.302	3.298	3.320	3.248	3.356	3.092
0.30	3.227	3.377	3.094	3.303	3.297	3.319	3.229	3.375	3.106
0.40	3.211	3.395	3.106	3.304	3.296	3.317	3.214	3.392	3.118
0.50	3.197	3.410	3.116	3.305	3.295	3.316	3.201	3.406	3.128
0.60	3.185	3.423	3.125	3.306	3.294	3.315	3.190	3.417	3.136
0.70	3.175	3.435	3.132	3.307	3.293	3.314	3.181	3.428	3.143
0.80	3.165	3.445	3.139	3.308	3.292	3.312	3.173	3.436	3.150
0.90	3.157	3.454	3.145	3.309	3.291	3.311	3.166	3.444	3.155
1.00	3.150		3.150	3.310		3.310	3.160		3.160

TABLE VII. Calculated structural parameters of Mo/A multilayers, where A is Fe, Ta, and W. The first column shows the relative concentration of material A in the multilayer. The in- and out-of-plane lattice constants are given in Å.

	Mo/Fe			Mo/Ta			Mo/W		
X	$a_{\parallel}^{\mathrm{Mo/Fe}}$	$a_{\perp}^{\mathrm{Mo}}$	$a_{\perp}^{\mathrm{Fe}}$	$a_{\parallel}^{\mathrm{Mo/Ta}}$	$a_{\perp}^{\mathrm{Mo}}$	$a_{\perp}^{\mathrm{Ta}}$	$a_{\parallel}^{\mathrm{Mo/W}}$	$a_{\perp}^{\mathrm{Mo}}$	$a_{\perp}^{\mathrm{W}}$
0.00	3.150	3.150		3.150	3.150		3.150	3.150	
0.10	3.138	3.158	2.579	3.158	3.145	3.503	3.151	3.149	3.167
0.20	3.125	3.168	2.593	3.166	3.138	3.491	3.152	3.148	3.166
0.30	3.109	3.179	2.608	3.176	3.131	3.479	3.153	3.148	3.165
0.40	3.091	3.192	2.626	3.187	3.124	3.464	3.154	3.147	3.165
0.50	3.070	3.206	2.648	3.200	3.114	3.448	3.155	3.146	3.164
0.60	3.045	3.224	2.674	3.215	3.104	3.429	3.156	3.146	3.163
0.70	3.015	3.245	2.706	3.232	3.091	3.406	3.157	3.145	3.162
0.80	2.978	3.270	2.747	3.253	3.076	3.380	3.158	3.144	3.161
0.90	2.931	3.301	2.799	3.278	3.058	3.349	3.159	3.144	3.161
1.00	2.870		2.870	3.310		3.310	3.160		3.160

Even so, the model is in good agreement with experimental structures, for example, in the case of Fe/V multilayers[7] but also for other systems. Liebig *et al.*[19] reported experimental in- and average out-of-plane lattice parameter of 2.977 Å and 3.016 Å, respectively, for a V/Cr multilayer with relative thickness, X, of 0.47, while our model in this case yields 2.916 Å and 3.009 Å for the in- and average out-of-plane lattice constants, respectively. For V/Mo multilayers with $X = 0.354$, Birch *et al.*[20] have reported in-plane lattice parameters of 3.05–3.09 Å and evaluated out-of-plane lattice parameters of 2.98 Å for the V layers and 3.09 Å for the Mo layers. Our model yields in this case 3.105 Å for the in-plane lattice parameter and 2.908 Å for the out-of-plane lattice parameter of the V layers and 3.182 Å for the in-plane lattice parameter of the Mo layers. As represented by these examples, the model yields lattice parameters that are in good agreement with experimental structures with a maximum deviation of less than 0.092 Å.

Birch *et al.*[21] have also reported epitaxial growth of V/Mo multilayers with various superlattice periodicities, Λ (see Fig. 1), with Λ ranging from 1.3 to 10.0 nm for systems with relative Mo concentration, X, of 0.5. From these data the evaluated average out-of-plane lattice parameters are 3.00 Å ($\Lambda = 5.0, 7.2$, and 10.0 nm) to 3.25 Å ($\Lambda = 1.3$ nm) depending on the periodicity. The result obtained using our model, presented in Table III, is, in this case, 3.025 Å. Considering that the agreement is significantly better for the multilayers with larger periodicities confirms our expectation that the model is more accurate for systems where the individual layers are thicker.

TABLE VIII. Calculated structural parameters of Ta/A multilayers, where A is Fe and W. The first column shows the relative concentration of material A in the multilayer. The in- and out-of-plane lattice constants is given in Å.

	Ta/Fe			Ta/W		
X	$a_{\parallel}^{\mathrm{Ta/Fe}}$	$a_{\perp}^{\mathrm{Ta}}$	$a_{\perp}^{\mathrm{Fe}}$	$a_{\parallel}^{\mathrm{Ta/W}}$	$a_{\perp}^{\mathrm{Ta}}$	$a_{\perp}^{\mathrm{W}}$
0.00	3.310	3.310		3.310	3.310	
0.10	3.270	3.358	2.454	3.278	3.349	3.068
0.20	3.230	3.409	2.491	3.253	3.380	3.087
0.30	3.189	3.462	2.530	3.233	3.405	3.103
0.40	3.146	3.518	2.571	3.217	3.425	3.115
0.50	3.103	3.577	2.614	3.204	3.443	3.126
0.60	3.059	3.639	2.660	3.192	3.457	3.135
0.70	3.013	3.704	2.708	3.182	3.470	3.142
0.80	2.967	3.774	2.759	3.174	3.481	3.149
0.90	2.919	3.847	2.813	3.167	3.491	3.155
1.00	2.870		2.870	3.160		3.160

Hence, we have demonstrated the ability to predict the geometry of a large group of multilayers using the model theory outlined here. We therefore provide calculated data using our model for a large number of different multilayers in Tables III to XVIII. The calculations have been performed using experimental elastic constants and lattice parameters given in Table I as input. In Tables III to VIII, we show the values predicted using our model of the in-plane and out-of-plane lattice parameters of multilayers composed of body-centered cubic metals from the transition metal series. The face-centered cubic based materials are shown in Tables IX to XVI, for various combinations of 3*d*, 4*d*, and 5*d* elements from the transition metals. In this study, we have chosen not to include the simple metals as well as any of the rare-earth elements. Finally, we display the geometry of Si-based multilayers in Tables XVII and XVIII. The data shown in Tables III to XVIII serves as a structural database.

In Tables III to XVIII we show the in- and out-of-plane lattice parameters for each component as well as the relative concentration of material B in each respective case. The average out-of-plane lattice parameter, $\langle a_{\perp} \rangle$, is not given explicitly but can easily be calculated by rewriting Eq. (9) so

$$\langle a_{\perp} \rangle = (1 - X)a_{\perp}^{A} + Xa_{\perp}^{B} \tag{10}$$

and by using the information provided in Tables III to XVIII.

When regarding the structural parameters in Tables III to XVIII, we note that a linear dependence of the different lattice parameters as the relative concentration in the multilayer varies is not to be expected unless the tetragonal shear constant and bulk modulus in the different components are very similar. A perfect linear behavior is, however, never achieved, even

TABLE IX. Calculated structural parameters of Ni/A multilayers, where A is Cu, Pd, Ag, Pt, and Au. The first column shows the relative concentration of material A in the multilayer. The in- and out-of-plane lattice constants are given in Å.

	Ni/Cu			Ni/Pd			Ni/Ag			Ni/Pt			Ni/Au		
X	$a_{\parallel}^{\mathrm{Ni/Cu}}$	$a_{\perp}^{\mathrm{Ni}}$	$a_{\perp}^{\mathrm{Cu}}$	$a_{\parallel}^{\mathrm{Ni/Pd}}$	$a_{\perp}^{\mathrm{Ni}}$	$a_{\perp}^{\mathrm{Pd}}$	$a_{\parallel}^{\mathrm{Ni/Ag}}$	$a_{\perp}^{\mathrm{Ni}}$	$a_{\perp}^{\mathrm{Ag}}$	$a_{\parallel}^{\mathrm{Ni/Pt}}$	$a_{\perp}^{\mathrm{Ni}}$	$a_{\perp}^{\mathrm{Pt}}$	$a_{\parallel}^{\mathrm{Ni/Au}}$	$a_{\perp}^{\mathrm{Ni}}$	$a_{\perp}^{\mathrm{Au}}$
0.00	3.520	3.520		3.520	3.520		3.520	3.520		3.520	3.520		3.520	3.520	
0.10	3.525	3.514	3.737	3.544	3.492	4.505	3.542	3.494	5.111	3.564	3.468	4.506	3.542	3.493	5.212
0.20	3.530	3.508	3.728	3.569	3.462	4.453	3.568	3.464	5.053	3.607	3.418	4.427	3.568	3.463	5.146
0.30	3.536	3.500	3.719	3.597	3.430	4.399	3.597	3.430	4.988	3.649	3.371	4.352	3.598	3.429	5.072
0.40	3.543	3.492	3.709	3.627	3.395	4.340	3.632	3.391	4.913	3.691	3.326	4.280	3.632	3.390	4.987
0.50	3.551	3.483	3.697	3.661	3.358	4.278	3.673	3.345	4.828	3.731	3.283	4.212	3.673	3.345	4.890
0.60	3.560	3.473	3.684	3.697	3.318	4.211	3.722	3.292	4.728	3.770	3.241	4.148	3.722	3.292	4.777
0.70	3.569	3.462	3.669	3.738	3.275	4.139	3.783	3.228	4.610	3.809	3.202	4.087	3.783	3.229	4.646
0.80	3.581	3.448	3.652	3.783	3.228	4.062	3.859	3.152	4.470	3.847	3.164	4.029	3.858	3.153	4.491
0.90	3.594	3.433	3.633	3.833	3.177	3.980	3.958	3.057	4.300	3.884	3.128	3.973	3.954	3.061	4.305
1.00	3.610		3.610	3.890		3.890	4.090		4.090	3.920		3.920	4.080		4.080

if the elastic constants are identical. Also, for those cases where the differences in the bulk lattice parameters between the components are small, as in the case of Fe/Cr multilayers, the variations in the lattice constants depending on the relative thickness in the multilayer are also small. Even so, the behavior of the variations discussed previously is still present, although in order to see those changes a much higher accuracy in the lattice constants is required.

TABLE X. Calculated structural parameters of Cu/A multilayers, where A is Pd, Ag, Pt, and Au. The first column shows the relative concentration of material A in the multilayer. The in- and out-of-plane lattice constants are given in Å.

	Cu/Pd			Cu/Ag			Cu/Pt			Cu/Au		
X	$a_{\parallel}^{\mathrm{Cu/Pd}}$	$a_{\perp}^{\mathrm{Cu}}$	$a_{\perp}^{\mathrm{Pd}}$	$a_{\parallel}^{\mathrm{Cu/Ag}}$	$a_{\perp}^{\mathrm{Cu}}$	$a_{\perp}^{\mathrm{Ag}}$	$a_{\parallel}^{\mathrm{Cu/Pt}}$	$a_{\perp}^{\mathrm{Cu}}$	$a_{\perp}^{\mathrm{Pt}}$	$a_{\parallel}^{\mathrm{Cu/Au}}$	$a_{\perp}^{\mathrm{Cu}}$	$a_{\perp}^{\mathrm{Au}}$
0.00	3.610	3.610		3.610	3.610		3.610	3.610		3.610	3.610	
0.10	3.642	3.564	4.312	3.644	3.561	4.887	3.669	3.527	4.317	3.645	3.561	4.957
0.20	3.673	3.521	4.255	3.681	3.510	4.810	3.717	3.461	4.235	3.681	3.510	4.871
0.30	3.703	3.480	4.200	3.720	3.457	4.732	3.758	3.408	4.169	3.720	3.457	4.782
0.40	3.733	3.441	4.149	3.762	3.402	4.650	3.792	3.365	4.114	3.762	3.402	4.690
0.50	3.761	3.404	4.100	3.807	3.345	4.565	3.821	3.328	4.069	3.807	3.346	4.596
0.60	3.788	3.369	4.054	3.855	3.286	4.477	3.846	3.297	4.030	3.854	3.287	4.498
0.70	3.815	3.335	4.010	3.907	3.224	4.386	3.868	3.271	3.997	3.905	3.227	4.398
0.80	3.841	3.304	3.968	3.963	3.160	4.291	3.887	3.247	3.968	3.959	3.164	4.295
0.90	3.866	3.273	3.928	4.024	3.093	4.192	3.905	3.227	3.942	4.017	3.100	4.189
1.00	3.890		3.890	4.090		4.090	3.920		3.920	4.080		4.080

TABLE XI. Calculated structural parameters of Rh/A multilayers, where A is Ni, Cu, Pd, and Ag. The first column shows the relative concentration of material A in the multilayer. The in- and out-of-plane lattice constants are given in Å.

	Rh/Ni			Rh/Cu			Rh/Pd			Rh/Ag		
X	$a_{\parallel}^{\mathrm{Rh/Ni}}$	$a_{\perp}^{\mathrm{Rh}}$	$a_{\perp}^{\mathrm{Ni}}$	$a_{\parallel}^{\mathrm{Rh/Cu}}$	$a_{\perp}^{\mathrm{Rh}}$	$a_{\perp}^{\mathrm{Cu}}$	$a_{\parallel}^{\mathrm{Rh/Pd}}$	$a_{\perp}^{\mathrm{Rh}}$	$a_{\perp}^{\mathrm{Pd}}$	$a_{\parallel}^{\mathrm{Rh/Ag}}$	$a_{\perp}^{\mathrm{Rh}}$	$a_{\perp}^{\mathrm{Ag}}$
0.00	3.800	3.800		3.800	3.800		3.800	3.800		3.800	3.800	
0.10	3.785	3.814	3.225	3.795	3.805	3.359	3.803	3.797	4.029	3.806	3.795	4.567
0.20	3.769	3.830	3.242	3.788	3.811	3.367	3.807	3.793	4.023	3.813	3.788	4.555
0.30	3.750	3.847	3.261	3.781	3.818	3.377	3.811	3.790	4.016	3.821	3.780	4.539
0.40	3.729	3.867	3.283	3.772	3.826	3.389	3.816	3.785	4.008	3.831	3.771	4.520
0.50	3.706	3.889	3.308	3.761	3.837	3.403	3.821	3.780	3.998	3.845	3.758	4.496
0.60	3.679	3.915	3.337	3.747	3.850	3.421	3.829	3.773	3.987	3.862	3.742	4.464
0.70	3.648	3.945	3.372	3.728	3.868	3.446	3.838	3.765	3.972	3.887	3.720	4.421
0.80	3.612	3.980	3.412	3.703	3.892	3.480	3.850	3.753	3.953	3.922	3.687	4.360
0.90	3.570	4.021	3.460	3.667	3.927	3.529	3.866	3.738	3.927	3.980	3.636	4.263
1.00	3.520		3.520	3.610		3.610	3.890		3.890	4.090		4.090

TABLE XII. Calculated structural parameters of Rh/A multilayers, where A is Ir, Pt, and Au. The first column shows the relative concentration of material A in the multilayer. The in- and out-of-plane lattice constants are given in Å.

	Rh/Ir			Rh/Pt			Rh/Au		
X	$a_{\parallel}^{\mathrm{Rh/Ir}}$	$a_{\perp}^{\mathrm{Rh}}$	$a_{\perp}^{\mathrm{Ir}}$	$a_{\parallel}^{\mathrm{Rh/Pt}}$	$a_{\perp}^{\mathrm{Rh}}$	$a_{\perp}^{\mathrm{Pt}}$	$a_{\parallel}^{\mathrm{Rh/Au}}$	$a_{\perp}^{\mathrm{Rh}}$	$a_{\perp}^{\mathrm{Au}}$
0.00	3.800	3.800		3.800	3.800		3.800	3.800	
0.10	3.806	3.795	3.869	3.807	3.793	4.090	3.806	3.794	4.595
0.20	3.811	3.790	3.865	3.815	3.786	4.078	3.813	3.788	4.580
0.30	3.815	3.786	3.861	3.823	3.778	4.065	3.821	3.780	4.562
0.40	3.820	3.782	3.857	3.833	3.770	4.050	3.832	3.770	4.541
0.50	3.824	3.778	3.854	3.843	3.760	4.034	3.845	3.758	4.513
0.60	3.827	3.774	3.850	3.855	3.749	4.017	3.863	3.741	4.478
0.70	3.831	3.771	3.848	3.868	3.737	3.997	3.887	3.719	4.430
0.80	3.834	3.768	3.845	3.883	3.723	3.974	3.922	3.687	4.363
0.90	3.837	3.765	3.842	3.900	3.708	3.949	3.978	3.637	4.259
1.00	3.840		3.840	3.920		3.920	4.080		4.080

We also want to note that, even though the structural variations in the different materials are considerable for a number of cases in Tables III to XVIII, such as, for example, in the Fe/Ta, Ni/Ag, or Ni/Au multilayers, with a respectable change in the c/a ratio, a transition from body-centered cubic to face-centered cubic structure or vice versa following Bain's path in any multilayer component is not obtained through any of the multilayer structures presented. For such a transition

TABLE XIII. Calculated structural parameters of Pd/A multilayers, where A is Ag, Pt, and Au. The first column shows the relative concentration of material A in the multilayer. The in- and out-of-plane lattice constants are given in Å.

	Pd/Ag			Pd/Pt			Pd/Au		
X	$a_{\parallel}^{\mathrm{Pd/Ag}}$	$a_{\perp}^{\mathrm{Pd}}$	$a_{\perp}^{\mathrm{Ag}}$	$a_{\parallel}^{\mathrm{Pd/Pt}}$	$a_{\perp}^{\mathrm{Pd}}$	$a_{\perp}^{\mathrm{Pt}}$	$a_{\parallel}^{\mathrm{Pd/Au}}$	$a_{\perp}^{\mathrm{Pd}}$	$a_{\perp}^{\mathrm{Au}}$
0.00	3.890	3.890		3.890	3.890		3.890	3.890	
0.10	3.902	3.871	4.394	3.895	3.882	3.956	3.902	3.871	4.403
0.20	3.916	3.850	4.371	3.899	3.876	3.950	3.915	3.851	4.378
0.30	3.930	3.828	4.346	3.903	3.870	3.945	3.929	3.830	4.350
0.40	3.946	3.804	4.319	3.906	3.865	3.940	3.945	3.806	4.321
0.50	3.964	3.778	4.289	3.909	3.860	3.936	3.962	3.781	4.289
0.60	3.984	3.749	4.257	3.912	3.856	3.932	3.981	3.754	4.254
0.70	4.006	3.718	4.221	3.914	3.853	3.928	4.002	3.724	4.217
0.80	4.031	3.683	4.182	3.916	3.850	3.925	4.025	3.691	4.175
0.90	4.058	3.644	4.139	3.918	3.847	3.923	4.051	3.655	4.130
1.00	4.090		4.090	3.920		3.920	4.080		4.080

TABLE XIV. Calculated structural parameters of Ir/A multilayers, where A is Ni, Cu, and Pd. The first column shows the relative concentration of material A in the multilayer. The in- and out-of-plane lattice constants are given in Å.

	Ir/Ni			Ir/Cu			Ir/Pd		
X	$a_{\parallel}^{\mathrm{Ir/Ni}}$	$a_{\perp}^{\mathrm{Ir}}$	$a_{\perp}^{\mathrm{Ni}}$	$a_{\parallel}^{\mathrm{Ir/Cu}}$	$a_{\perp}^{\mathrm{Ir}}$	$a_{\perp}^{\mathrm{Cu}}$	$a_{\parallel}^{\mathrm{Ir/Pd}}$	$a_{\perp}^{\mathrm{Ir}}$	$a_{\perp}^{\mathrm{Pd}}$
0.00	3.840	3.840		3.840	3.840		3.840	3.840	
0.10	3.828	3.850	3.181	3.836	3.844	3.308	3.841	3.839	3.967
0.20	3.814	3.861	3.195	3.830	3.848	3.315	3.843	3.838	3.965
0.30	3.799	3.875	3.211	3.824	3.854	3.323	3.844	3.836	3.962
0.40	3.780	3.890	3.230	3.816	3.860	3.333	3.846	3.835	3.959
0.50	3.758	3.909	3.254	3.805	3.869	3.346	3.849	3.833	3.955
0.60	3.730	3.932	3.282	3.791	3.881	3.364	3.852	3.830	3.949
0.70	3.697	3.960	3.318	3.772	3.897	3.388	3.857	3.826	3.942
0.80	3.654	3.997	3.366	3.744	3.920	3.425	3.863	3.821	3.932
0.90	3.597	4.044	3.429	3.698	3.959	3.486	3.873	3.813	3.917
1.00	3.520		3.520	3.610		3.610	3.890		3.890

TABLE XV. Calculated structural parameters of Ir/A multilayers, where A is Ag, Pt, and Au. The first column shows the relative concentration of material A in the multilayer. The in- and out-of-plane lattice constants are given in Å.

	Ir/Ag			Ir/Pt			Ir/Au		
X	$a_{\parallel}^{\mathrm{Ir/Ag}}$	$a_{\perp}^{\mathrm{Ir}}$	$a_{\perp}^{\mathrm{Ag}}$	$a_{\parallel}^{\mathrm{Ir/Pt}}$	$a_{\perp}^{\mathrm{Ir}}$	$a_{\perp}^{\mathrm{Pt}}$	$a_{\parallel}^{\mathrm{Ir/Au}}$	$a_{\perp}^{\mathrm{Ir}}$	$a_{\perp}^{\mathrm{Au}}$
0.00	3.840	3.840		3.840	3.840		3.840	3.840	
0.10	3.843	3.837	4.498	3.843	3.837	4.034	3.843	3.837	4.517
0.20	3.848	3.834	4.491	3.847	3.834	4.028	3.848	3.834	4.509
0.30	3.853	3.829	4.482	3.851	3.831	4.022	3.853	3.829	4.498
0.40	3.859	3.824	4.470	3.856	3.826	4.014	3.859	3.824	4.485
0.50	3.868	3.817	4.455	3.862	3.822	4.005	3.868	3.817	4.468
0.60	3.879	3.807	4.434	3.869	3.816	3.995	3.880	3.807	4.445
0.70	3.896	3.793	4.404	3.878	3.809	3.982	3.897	3.793	4.412
0.80	3.923	3.771	4.358	3.888	3.800	3.966	3.923	3.771	4.361
0.90	3.972	3.731	4.276	3.902	3.788	3.946	3.971	3.732	4.273
1.00	4.090		4.090	3.920		3.920	4.080		4.080

to occur, it is required to have a smaller relative amount of, for example, Ni in Ni/Ag or Ni/Au from what is shown in Table IX or to grow multilayers of different materials, which are not considered here, where the components have a considerable size difference and where one of the components are considerably stiffer than the other.

TABLE XVI. Calculated structural parameters of Ag/A multilayers, where A is Pt and Au, and of Pt/Au multilayers. The first column shows the relative concentration of material A in the multilayer. The in- and out-of-plane lattice constants are given in Å.

	Ag/Pt			Ag/Au			Pt/Au		
X	$a_{\parallel}^{\mathrm{Ag/Pt}}$	$a_{\perp}^{\mathrm{Ag}}$	$a_{\perp}^{\mathrm{Pt}}$	$a_{\parallel}^{\mathrm{Ag/Au}}$	$a_{\perp}^{\mathrm{Ag}}$	$a_{\perp}^{\mathrm{Au}}$	$a_{\parallel}^{\mathrm{Pt/Au}}$	$a_{\perp}^{\mathrm{Pt}}$	$a_{\perp}^{\mathrm{Au}}$
0.00	4.090	4.090		4.090	4.090		3.920	3.920	
0.10	4.047	4.157	3.744	4.089	4.092	4.065	3.926	3.912	4.357
0.20	4.016	4.205	3.785	4.088	4.093	4.067	3.932	3.902	4.345
0.30	3.993	4.242	3.816	4.087	4.095	4.068	3.940	3.891	4.330
0.40	3.976	4.270	3.841	4.086	4.096	4.070	3.949	3.878	4.313
0.50	3.962	4.293	3.860	4.085	4.098	4.072	3.960	3.862	4.292
0.60	3.950	4.312	3.877	4.084	4.099	4.073	3.974	3.843	4.267
0.70	3.941	4.328	3.890	4.083	4.101	4.075	3.991	3.820	4.237
0.80	3.933	4.342	3.902	4.082	4.102	4.077	4.012	3.791	4.198
0.90	3.926	4.354	3.911	4.081	4.104	4.078	4.041	3.753	4.148
1.00	3.920		3.920	4.080		4.080	4.080		4.080

TABLE XVII. Calculated structural parameters of Si/A multilayers, where A is Ge, GaAs, InP, and InAs. The first column shows the relative concentration of material A in the multilayer. The in- and out-of-plane lattice constants are given in Å.

	Si/Ge			Si/GaAs			Si/InP			Si/InAs		
X	$a_{\parallel}^{\mathrm{Si/Ge}}$	$a_{\perp}^{\mathrm{Si}}$	$a_{\perp}^{\mathrm{Ge}}$	$a_{\parallel}^{\mathrm{Si/GaAs}}$	$a_{\perp}^{\mathrm{Si}}$	$a_{\perp}^{\mathrm{GaAs}}$	$a_{\parallel}^{\mathrm{Si/InP}}$	$a_{\perp}^{\mathrm{Si}}$	$a_{\perp}^{\mathrm{InP}}$	$a_{\parallel}^{\mathrm{Si/InAs}}$	$a_{\perp}^{\mathrm{Si}}$	$a_{\perp}^{\mathrm{InAs}}$
0.00	5.431	5.431		5.431	5.431		5.431	5.431		5.431	5.431	
0.10	5.449	5.417	5.801	5.447	5.418	5.841	5.456	5.411	6.357	5.462	5.407	6.765
0.20	5.468	5.402	5.789	5.464	5.405	5.825	5.484	5.390	6.322	5.497	5.380	6.720
0.30	5.488	5.386	5.775	5.483	5.391	5.808	5.514	5.366	6.284	5.536	5.349	6.671
0.40	5.509	5.370	5.761	5.502	5.375	5.790	5.548	5.340	6.243	5.580	5.315	6.616
0.50	5.531	5.353	5.746	5.523	5.359	5.771	5.586	5.310	6.197	5.631	5.276	6.553
0.60	5.554	5.335	5.730	5.545	5.342	5.751	5.629	5.277	6.146	5.689	5.230	6.482
0.70	5.578	5.316	5.713	5.569	5.323	5.729	5.677	5.240	6.089	5.758	5.178	6.400
0.80	5.603	5.297	5.696	5.595	5.303	5.706	5.731	5.198	6.024	5.839	5.116	6.305
0.90	5.630	5.276	5.677	5.623	5.282	5.680	5.795	5.150	5.952	5.937	5.042	6.192
1.00	5.658		5.658	5.653		5.653	5.869		5.869	6.058		6.058

TABLE XVIII. Calculated structural parameters of Si/A multilayers, where A is InSb, GaP, and (Ga,In)As. The first column shows the relative concentration of material A in the multilayer. The in- and out-of-plane lattice constants are given in Å. (Ga,In)As is an alloyed semiconductor with chemical formula $Ga_{0.47}In_{0.53}As$

	Si/InSb			Si/GaP			Si/(Ga,In)As		
X	$a_{\parallel}^{\mathrm{Si/InSb}}$	$a_{\perp}^{\mathrm{Si}}$	$a_{\perp}^{\mathrm{InSb}}$	$a_{\parallel}^{\mathrm{Si/GaP}}$	$a_{\perp}^{\mathrm{Si}}$	$a_{\perp}^{\mathrm{GaP}}$	$a_{\parallel}^{\mathrm{Si/(Ga,In)As}}$	$a_{\perp}^{\mathrm{Si}}$	$a_{\perp}^{\mathrm{(Ga,In)As}}$
0.00	5.431	5.431		5.431	5.431		5.431	5.431	
0.10	5.474	5.397	7.736	5.433	5.430	5.466	5.458	5.410	6.289
0.20	5.524	5.359	7.666	5.434	5.428	5.465	5.487	5.387	6.258
0.30	5.580	5.315	7.588	5.436	5.427	5.463	5.519	5.363	6.225
0.40	5.646	5.264	7.498	5.438	5.426	5.462	5.554	5.335	6.188
0.50	5.723	5.204	7.394	5.440	5.424	5.460	5.592	5.305	6.148
0.60	5.816	5.134	7.273	5.442	5.423	5.458	5.635	5.272	6.103
0.70	5.928	5.049	7.129	5.444	5.421	5.456	5.683	5.235	6.054
0.80	6.067	4.946	6.956	5.446	5.419	5.454	5.737	5.194	6.000
0.90	6.244	4.818	6.744	5.448	5.418	5.453	5.799	5.147	5.938
1.00	6.479		6.479	5.451		5.451	5.869		5.869

IV. SUMMARY AND CONCLUSIONS

We have, using a simple analytical model based on the theory of elasticity, calculated the lattice parameters and thereby the structure of a wide range of metal and semiconductor multilayer structures. The model is shown to be in good agreement with first-principles calculations. The structure variations for the multilayer components are, in general, found not to be volume preserving nor does it preserve a cubic symmetry. The deviation from a linear dependence with varying composition is also explained by the difference in elastic constants of the constituting elements of the multilayers. By comparing experimental data for systems with varying periodicities it is also shown that the model is more appropriate in describing thicker multilayers with larger periodicities. We conclude that the model has predictive power, yielding structural parameters that are in quantitative agreement with first-principles calculations, while at the same time keeping the computations to a minimum, for example, the results shown in Fig. 2 was obtained within seconds on a regular workstation. Furthermore, we note that even though the theory outlined here is valid for multilayers with interfaces being any of the (100), (010), or (001) surfaces and based on cubic materials, the methodology can be adjusted to be valid for any type of crystal structure and growth direction. With the predicted geometries of a large number of multilayers we hope to shed light on the experimental growth of such systems and the mechanisms that govern their structures.

ACKNOWLEDGMENTS

We wish to acknowledge the Swedish Research Council, SSF, KAW, and ERC (grant 247062-ASD) for financial support. First-principles calculations were made possible due to computational resources provided by the Swedish National Infrastructure for Computing.

*mikael.rasander@gmail.com

[1] M. N. Baibich, J. M. Broto, A. Fert, F. NguyenVan Dau, F. Petroff, P. Etienne, G. Creuzet, A. Friederich, and J. Chazelas, Phys. Rev. Lett. **61**, 2472 (1988).

[2] P. Grünberg, R. Schreiber, Y. Pang, M. B. Brodsky, and H. Sowers, Phys. Rev. Lett. **57**, 2442 (1986).

[3] H. W. Hugosson, U. Jansson, B. Johansson, and O. Eriksson, Science **293**, 2434 (2001).

[4] M. Kelly, *Low-Dimensional Semiconductors* (Clarendon Press, Oxford, UK, 1995).

[5] A. Höglund, O. Eriksson, C. W. M. Castleton, and S. Mirbt, Phys. Rev. Lett. **100**, 105501 (2008).

[6] H. L. Skriver, Phys. Rev. B **31**, 1909 (1985).

[7] A. Broddefalk, P. Nordblad, P. Blomquist, P. Isberg, R. Wäppling, O. Le Bacq, and O. Eriksson, J. Magn. Magn Mater. **241**, 260 (2002).

[8] O. Eriksson, L. Bergqvist, E. Holmström, A. Bergman, O. Le Bacq, S. Frota-Pessoa, B. Hjörvarsson, and L. Nordström, J. Phys. Condens. Matter **15**, S599 (2003).

[9] N. W. Ashcroft and N. D. Mermin, *Solid State Physics* (Thomson Learning Inc., New York, 1976).

[10] G. Simmons and H. Wang, *Single Crystal Elastic Constants and Calculated Aggregate Properties: A Handbook*, 2nd ed. (The MIT Press, Cambridge, MA, 1971).

[11] L. Vegard, Z. Phys. **5**, 17 (1921).

[12] G. Kresse and J. Furthmüller, Phys. Rev. B **54**, 11169 (1996).

[13] G. Kresse and D. Joubert, Phys. Rev. B **59**, 1758 (1999).

[14] P. E. Blöchl, Phys. Rev. B **50**, 17953 (1994).

[15] J. P. Perdew, K. Burke, and M. Ernzerhof, Phys. Rev. Lett. **77**, 3865 (1996).

[16]L. Fast, J. M. Wills, B. Johansson, and O. Eriksson, Phys. Rev. B **51**, 17431 (1995).
[17]L. Koči, Y. Ma, A. R. Oganov, P. Souvatzis, and R. Ahuja, Phys. Rev. B **77**, 214101 (2008).
[18]P. Söderlind, R. Ahuja, O. Eriksson, J. M. Wills, and B. Johansson, Phys. Rev. B **50**, 5918 (1994).
[19]A. Liebig, G. Andersson, J. Birch, and B. Hjörvarsson, Thin Solid Films **516**, 8468 (2008).
[20]J. Birch, J.-E. Sundgren, and P. F. Fewster, J. Appl. Phys. **78**, 6562 (1995).
[21]J. Birch, L. Hultman, J.-E. Sundgren, and G. Radnoczi, Phys. Rev. B **53**, 8114 (1996).